Cuadernos de Investigación Geográfica *Geographical Research Letters*	2026	Nº 52 (2)	pp. 23-48	EISSN 1697-9540

http://doi.org/10.18172/cig.7019

RAINFALL PATTERN AND EROSIVITY: A 90-YEAR STUDY IN A CROPLAND REGION OF ARGENTINA

MARIELA SOLEDAD SEEHAUS[1,2]*, MANUEL LÓPEZ-VICENTE[3], ANA BEATRIZ WINGEYER[2], MARIA CAROLINA SASAL[2], ALEJANDRA LORENA CUATRIN[2], EMANUEL MELGARES[2]

[1] *Group Aquaterra, Universidade da Coruña, 15071 A Coruña, Spain.*

[2] *Instituto Nacional de Tecnología Agropecuaria – EEA Paraná, Ruta 11, km. 12.5. 3100 Paraná, Entre Ríos, Argentina.*

[3] *GEOFOREST, Departamento de Ciencias Agrarias y del Medio Natural, Escuela Politécnica Superior de Huesca, Instituto Universitario de Investigación en Ciencias Ambientales de Aragón (IUCA), Universidad de Zaragoza, 22071 Huesca, Spain.*

ABSTRACT. Water soil erosion is a significant threat to agricultural sustainability and a key process of land degradation. Climate change is altering precipitation patterns and increasing rainfall erosivity globally, leading to more extreme hydrological conditions, yet many agriculturally significant regions lack detailed long-term analysis. This study addresses this gap by quantifying 90-year trends (1934–2023) in key precipitation metrics—total depth, number of rainy days, heavy rainfall (% of rainfall ≥ 50 mm), and rainfall erosivity (R-factor)—in a critical cropland region of Argentina. Analysis of daily data from the Paraná Agrometeorological Station revealed significant breakpoints in the 1970s. Post-breakpoint increases were observed for annual rainfall depth (+16% since 1975), rainy days (+19% since 1972), heavy rainfall events (+21% since 1971), and rainfall erosivity (+24% since 1977). On a monthly basis, March exhibited the highest erosivity. Despite a recent decrease in total monthly precipitation for March, its erosive potential appears to be sustained by a higher concentration of rainfall in intense events. Conversely, the period from May to September was characterized by lower and more stable erosivity values. Positives and significant correlations were established between the El Niño-Southern Oscillation (ENSO), measured by the Oceanic Niño Index (ONI), and all rainfall variables, with the strongest influence observed during the spring-summer seasons for rainfall depth (r= 0.24 to 0.51). Furthermore, the frequency of quarters classified as El Niño conditions has increased about 91% since the mid-1970s breakpoint. This study demonstrates a clear climatic shift towards conditions of higher precipitation and greater erosivity in the region. These findings underscore the urgent need for enhanced soil and water conservation policies to mitigate the increasing risk of land degradation.

Patrones de precipitación y erosividad: un estudio de 90 años en una región agrícola de Argentina

RESUMEN. La erosión hídrica constituye uno de los principales procesos de degradación de suelos y representa una amenaza para la sostenibilidad de los sistemas agrícolas. En el contexto del cambio climático, se han observado modificaciones en los regímenes de precipitación y un incremento de la erosividad de las lluvias a escala global, lo que se traduce en una mayor recurrencia de condiciones hidrológicas extremas. No obstante, diversas regiones de relevancia agroproductiva aún presentan un vacío de conocimiento en relación con análisis sistemáticos de largo plazo. El presente estudio contribuye a subsanar esta limitación mediante la evaluación de las tendencias registradas durante un período de 90 años (1934-2023) en variables pluviométricas clave—precipitación total anual, número de días con precipitación, lluvias intensas (% de lluvia en eventos mayores a 50 mm) y erosividad de la lluvia (factor R)—en una región agrícola estratégica de Argentina. El análisis de datos diarios correspondientes a la Estación Agrometeorológica Paraná permitió identificar puntos de cambio significativos durante la década de 1970. Durante el segundo periodo identificado se registraron incrementos en la precipitación anual (+16 % desde 1975), en el número de días con lluvia (+19 % desde 1972), lluvias intensas (+21 % desde 1971) y en la erosividad de la lluvia (+24 % desde 1977). A escala mensual, marzo presentó los valores más elevados de erosividad. Si bien se observó una disminución reciente de la precipitación total mensual en dicho mes, el potencial erosivo se mantuvo elevado, probablemente como consecuencia de una mayor concentración de la precipitación en eventos de alta intensidad. En contraste, el período comprendido entre mayo y septiembre se caracterizó por valores de erosividad más bajos y una mayor estabilidad temporal. Asimismo, se determinó una correlación positiva y estadísticamente significativa entre el fenómeno El Niño–Oscilación del Sur (ENOS), cuantificado mediante el Índice Oceánico de El Niño (ONI), y el conjunto de variables pluviométricas analizadas, siendo la influencia más marcada durante las estaciones de primavera y verano. Adicionalmente, se constató un incremento en la frecuencia de trimestres clasificados bajo condiciones El Niño a partir del punto de cambio identificado a mediados de la década de 1970. Los resultados evidencian un desplazamiento del régimen climático regional hacia escenarios caracterizados por mayores precipitaciones y un incremento sostenido de la erosividad. Estos hallazgos refuerzan la necesidad de implementar y fortalecer estrategias integrales de conservación de suelos y agua, con el fin de reducir el riesgo creciente de degradación de suelos en la región.

Key words: rainfall, rainy days, heavy rainfall, rainfall erosivity, climate change.

Palabras clave: precipitación, días de lluvia, precipitación intensa, erosividad de la lluvia, cambio climático.

Received: 9 September 2025

Accepted: 22 January 2026

***Corresponding author:** Mariela Soledad Seehaus, *Group Aquaterra, Universidade da Coruña, 15071 A Coruña, Spain.* E-mail: seehaus.mariela@inta.gob.ar

1. Introduction

Rainfall erosivity is one of the most important parameters for describing soil erosion processes by water (López-Vicente *et al.*, 2008). The rainfall erosivity factor (R) is an index that describes the power of rainfall and runoff to cause soil detachment and transport and deposition (Renard *et al.*, 1997) and is calculated with rainfall depth and intensity records. At a global scale, Panagos *et al.* (2017) published the first global map with erosivity values estimated as R factors (based on the equation of the RUSLE2 model of soil erosion by water). The mean of the global R-factor map is 2190 MJ mm ha^{-1} h^{-1} yr^{-1} with high variability. For South America, the average R factor is 5874 MJ mm ha^{-1} h^{-1} yr^{-1}: Chile has the lowest value (1320 MJ mm ha^{-1} h^{-1} yr^{-1}), followed by Argentina (2232 MJ mm ha^{-1} h^{-1} yr^{-1}). The rest of the South American countries have high mean erosivity values (>3700 MJ mm ha^{-1} h^{-1} yr^{-1}). They reported that the spatial patterns of the highest erosivity values coincided with the corresponding patterns of extreme rainfall events. Therefore, R values present strong spatial and temporal variability, as they are linked to changes in precipitation parameters (Angulo-Martínez *et al.*, 2009).

In the current scenario of climate change, and using 2010 as a baseline, Panagos *et al.* (2022) estimated an increase in global rainfall erosivity between 26.2 and 28.8% for 2050 and 27–34.3% for 2070. Specifically for South America, they estimate an increase of 12.9% by 2050, which varies depending on the region considered. Over Brazil, Almagro *et al.* (2017) predicted significant increases (up to 109%) and decreases (as much as –71%) in rainfall erosivity for different parts of the country over the current century. These studies show that the R factor is changing globally due to climate change, but at the same time, the orientation and magnitude of the change differ across different regions of the planet.

On a global scale, the Intergovernmental Panel on Climate Change (2023) agrees that there is evidence of change in some extreme events from observations collected since 1950. Nevertheless, confidence in these data depends on the quality and quantity of the data, which vary across regions and for different variables. For precipitation, the global mean precipitation over continental surfaces is likely to have increased since 1950, with a more rapid rate of increase since the 1980s, but the statistical analysis has medium confidence. The frequency and intensity of heavy precipitation events have increased since the 1950s over most land areas for which observational data are sufficient for trend analysis. Similarly, a study at a global scale by Alexander *et al.* (2006) reported a general increase in precipitation indices for the 1979–2003 period concerning 1901-1950.

In Southeast South America, there were increasing trends in annual rainfall during the period 1950–2008 (Magrin *et al.*, 2014a), as well as a remarkable increase in the frequency of extreme precipitation over different thresholds ranging from 50-125 mm (Re and Barros, 2009). It is one of the few subregions where a robust positive trend in precipitation and significant intensification of heavy precipitation have been detected since the early 20th century with high confidence. A decade ago, Magrin *et al.* (2014a) predicted an increase of 25% in rainfall for this region by 2100. In addition, southern South America is one of the extratropical regions most affected by the El Niño/Southern Oscillation (ENSO) phenomenon (Grimm *et al.*, 2000). ENSO is one of the most important patterns of so-called interannual climate variability, which includes changes in the circulation of the atmosphere that can last from several months to a few years. During the so-called El Niño (EN) phenomenon, there is anomalous warming of the surface waters of the Central and Eastern Equatorial Pacific Ocean, and the sea surface temperature (SST) is then characterized by positive anomalies (SST> 0) and, inversely, La Niña (LN) (anomalous cooling of the same waters). Throughout EN, the region experiences positive precipitation anomalies during the spring and period from November to February of the following year, whereas during LN precipitation tends to decrease between June to December. However, Barros *et al.* (2008) suggested that this is true for the northern part of South America, but not for the southern part (south of 30°S).

Over most of the Argentine territory, positive trends in precipitation were observed from 1916–1991, especially since the 1950s (Barros *et al.*, 2000). In recent decades, the most important region suitable for agricultural production in Argentina ("Pampas region"), has experienced increases both in average values and in the frequency and intensity of occurrence of extreme climatic events (Magrin *et al.*, 2014b; Podestá *et al.*, 2009). Casas (2015) states that soil erosion increased during the period 1965-2015, with a marked increase since 1990, leading to soil degradation in agricultural areas of the country, especially in sloping areas of the humid Pampas and Mesopotamian regions (Casas, 2015).

In the province of Entre Ríos (Argentina), water erosion is an important problem (Sasal *et al.*, 2015). This is particularly relevant given that it is located within the "Pampas region" and ranks fourth in terms of the area planted with cereals and oilseeds in the country (Ministerio de Economía, 2023). However, the availability of meteorological information with high-resolution rainfall measurements at a small time step, needed to calculate the R factor, is generally not available, particularly over the large periods necessary to calculate the effects of climate change on precipitation parameters and depends on the study region. For these reasons, although there are studies on the Pampas region with the methodology of calculating R, there are an increasing number of studies that correlate and estimate erosivity on the basis of indices (Ares *et al.*, 2010; C.M. Di Leo *et al.*, 1999; Behrends Kraemer *et al.*, 2018; Maggi, 2002). For Entre Ríos, the R factor for 1950-2005 was obtained by Rojas and Conde (1985) and actualized by Saluso (2008): 6088 MJ mm ha^{-1} h^{-1} yr^{-1} (using the methodology proposed by USLE). Recently, Crettaz *et al.* (2016) applied the Modified Fournier Index and validated its use for the calculation of the R factor for the study area for the same period. In general, they reported an increase in precipitation and R factor values in recent decades. However, no study has calculated R in this region for dates before 1950 or after 2005.

To fill in this gap, this study involves a period of 90 years (1934-2023) in the area of influence of Paraná, Entre Ríos (Argentina) with the objective of identifying changes in precipitation and erosivity under the climate change scenario. The specific objectives were to i) evaluate annual and seasonal evolution of precipitation depth, number of rainy days and intense rainfall (≥ 50 mm), ii) estimate rainfall erosivity and characterize its annual and seasonal trend, and iii) evaluate the influence of ENSO on the four rainfall parameters. This study aids in improving the knowledge about the consequences of the current climate change on rainfall erosivity and soil degradation. In addition, our results will be of interest to farmers with respect to water availability and highlight the need to promote soil conservation policies against soil water erosion.

2. Materials and methods

2.1. Study area and data availability

The study was carried out at the Paraná Experimental Station of the Instituto Nacional de Tecnología Agropecuaria (INTA-Paraná) of Entre Ríos Province, Argentina (-31° 50' 55.7" S, -60° 32' 10.2" O). This study site was chosen because of the extensive temporal duration of the data series. Within the study region, it is the agrometeorological station with the longest series, with 90 years of uninterrupted data collection (Fig. 1).

The region has a subhumid and temperate climate with no dry season, which corresponds to the "Cfa" classification of Köppen (Peel, 2007). The latest report for this area, with a reference period of 30 years (1991-2020), revealed an average temperature of 18.8 °C and an average annual precipitation of 1102 mm (Wingeyer *et al.* 2022). The area is covered by a fine, illitic, thermic Aquic Argiudoll (US Soil Taxonomy) of the Tezanos Pinto Series (Luvic Phaeozem, WRB). The texture of the A horizon is silty loam with 27 and 66% of clay and silt, respectively (Plan Mapa de Suelos, 1998). This soil belongs to the order Mollisol, which represents approximately 25% of the total area of Entre Ríos and is used mainly for agriculture: cereal and oilseed crops (Gabioud, 2018). The main soil constraint to cropping is its susceptibility to water erosion due to a combination of various factors: intense rainfall, very long slopes (>500 m) with relatively low gradients, the silty texture of the topsoil and the low permeability of the B horizon of the Argiudolls (Sasal *et al.*, 2010).

Daily rainfall data from the Agrometeorological Station of INTA-Paraná corresponding to the period 1934–2023 was obtained from a type B rain gauge (Saluso, 1999). The estimated and analysed variables at the monthly and annual scales were as follow: rainfall depth (mm), number of rainy days (n), heavy rainfall (% of rainfall ≥ 50 mm), and rainfall erosivity (MJ mm ha^{-1} h^{-1} $month^{-1}$ or yr^{-1}). Heavy rainfall was calculated as a percentage of rainfall on days with ≥ 50 mm concerning the total rainfall (annual and monthly).

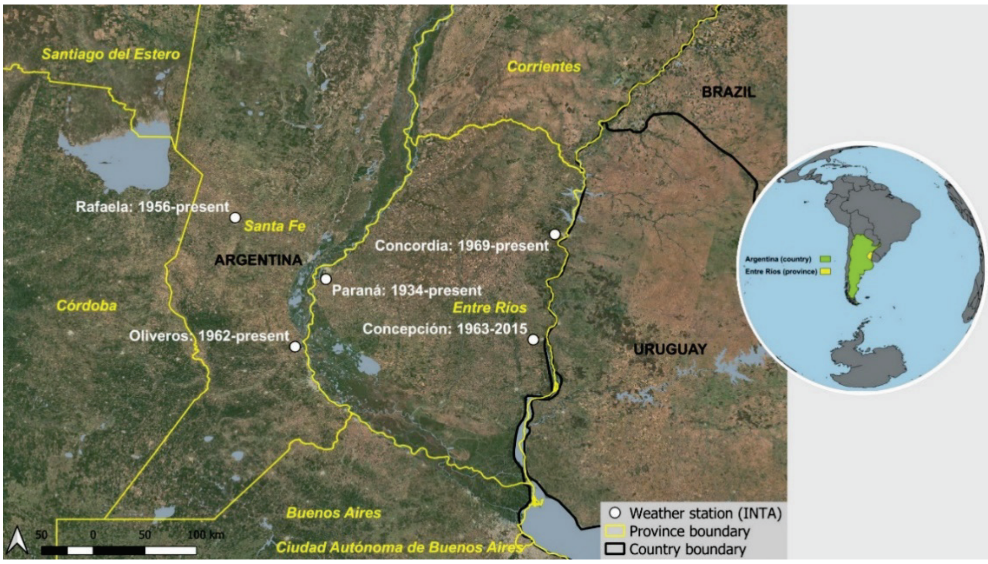

Figure 1. Location of the Agrometeorological Station of INTA-Paraná in Argentina and other meteorological stations with in the region, with the indication of the length of the available time series.

Considering the literature on the influence of the ENSO phenomenon in the area and to refine the analysis of rainfall parameters evolution, the ONI for the 1934-2023 period was calculated via the free available data at the website of the National Oceanic and Atmospheric Administration U.S. Department of Commerce (NOAA, 2024).

2.2. Assessment and validation of rainfall erosivity

The formulas for computing rainfall erosivity have changed over the years on the basis of new scientific results (Nearing *et al.*, 2017). The first equation was developed in 1958 by Wischmeier and Smith (involved in the Universal Soil Loss Equation (USLE)). They defined the erosivity of a rainfall event (***EI30***; MJ mm ha^{-1} h^{-1} $event^{-1}$) as a multiple of two factors: I) the rainfall energy of the storm (***E***; MJ ha^{-1} $event^{-1}$) and II) the maximum continuous 30-min intensity during an individual storm (***I30***; mm h^{-1}). Recently, the Revised Universal Soil Loss Equation version 2 (RUSLE2) (USDA-Agricultural Research Service, 2013) proposed the use of the following exponential equation (Equation 1):

$$e = 0.29\left(1 - 0.72exp(-0.082i)\right) \quad (1)$$

where ***e*** (MJ ha^{-1} mm^{-1}) is the energy of the rainfall per unit rainfall depth, and ***i*** (mm h^{-1}) is the rainfall intensity (mm h^{-1}) recorded according to the temporal resolution of the rain gauge.

The rainfall erosivity for an entire storm (*EI30*) includes a *n* number of records *r*, and is subsequently calculated as the sum of all *e* multiplied by the volume of rainfall registered during the *r* period (ΔV_r, mm) and multiplied by the maximum continuous 30-min rainfall intensity of the storm, *I30* (mm h^{-1}) (Equation 2):

$$EI_{30} = (\sum_{r=1}^{r=n} e_r \Delta V_r) I_{30} \quad (2)$$

Finally, the *R* factor is the sum of all *EI30* values obtained during one year. Given that the necessary records for calculating rainfall erosivity according to this methodology are not available for the entire study period (1934-2023) in the study area, *R* was estimated in accordance with the proposal of de Santos Loureiro and de Azevedo Coutinho (2001). These authors proposed an equation involving monthly rainfall for days with ≥10.0 mm (rain10) and the monthly number of days with rainfall ≥10.0 mm (days10) for the Algarve region in Portugal (Equation 3). This equation has the advantage of being applicable in places with daily rainfall values. It has been tested successfully in Italy (Diodato, 2004), Spain (López-Vicente *et al.*, 2011), northern Portugal (Bertocco *et al.*, 2025), the Mekong River Basin (Suif *et al.*, 2016), Poland (Halecki *et al.*, 2018), Georgia (Tsitsagi *et al.*, 2018) and Vietnam (Ranzi *et al.*, 2012).

$$R = \sum_{m=1}^{12} (7.05 \cdot rain10_m - 88.92 \cdot days10_m) \quad (3)$$

where m is the month.

To evaluate its robustness, validation was carried out with values obtained with the approach of R-RUSLE2, using available data from a shorter time series (1999-2023). For this purpose, we used 15-minute rainfall data obtained from a float-type rain gauge of the Agrometeorological Station of INTA-Paraná (Saluso, 1999). Despite the impossibility of validating the robustness of Eq. (3) for the first decades of our precipitation database, we assumed the validity of this equation in order to achieve the objective of this study. Then, erosivity was calculated via Equation (1) and (2).

Finally, the values of annual and monthly rainfall erosivity obtained through the two methodologies (exponential and linear) were correlated and evaluated.

2.3. Statistical analysis

2.3.1. Annual values and variability of rainfall parameters

The variables under study were analysed with descriptive statistics and correlation analysis (Pearson's coefficient). The statistical packages "strucchange" (Bai and Perron, 1998) and "changepoints" (Scott and Knott, 1974) with R software (version 4.4.0) (R Core Team, 2020) were used to identify breakpoints in time series data in the annual values of the four variables (rainfall depth, rainfall erosivity, number of rainy days and heavy rainfall). Before this, normal distribution of the data was checked. Bayesian Information Criterion (BIC) was used as a penalty to determine the breakpoints by considering the points of change in the mean and their location in the data series (Fearnhead, 2019).

2.3.2. Seasonal variability of rainfall parameters

To characterize the monthly and seasonal patterns of each variable of precipitation (*P*), and how these patterns evolved over the study period (T = 90 years), the relative differences ($\delta_{P,t,y}$) were calculated at each month *t* of each year *y* (equations 4a, b), and then, their mean relative difference ($MRD_{P,T}$) (equation 4c) and standard deviation of the relative difference ($SDRD_{P,T}$) (equation 4d) for the whole period were calculated. The combined analysis of MRD and SDRD has been useful for identifying patterns and their variability for any type of variable and is frequently used in soil science, especially for the evaluation of soil moisture and temperature dynamics (Vachaud *et al.*, 1985; Nolz and Loiskandl, 2017; Wei *et al.*, 2017; López-Vicente and Álvarez, 2018). These metrics are less common in time-series analysis of precipitation datasets, but MRD was successfully used by Henn *et al.* (2018) in the western United States, by Wang *et al.* (2019) in eastern China, and by Nordlund and Tuomenvirta (1998) in Finland.

$$\overline{P_y} = \frac{1}{12} \sum_{t=1}^{t=12} P_t \tag{4a}$$

$$\delta_{P,t,y} = \frac{P_t - \overline{P_y}}{\overline{P_y}} \tag{4b}$$

$$MRD_{P,T} = \frac{1}{90} \sum_{y=1}^{y=90} \delta_{P,t,y} \tag{4c}$$

$$SDRD_{P,T} = \sqrt{\frac{1}{89} \sum_{y=1}^{y=90} \left(\delta_{P,t,y} - MRD_{P,T}\right)^2} \tag{4d}$$

$$ITS_{P,T} = \sqrt{{MRD_{P,T}}^2 + {SDRD_{P,T}}^2} \tag{4e}$$

To refine the analysis of the temporal series, the index of the temporal stability (***$ITS_{P,T}$***) (equation 4e) was calculated for the whole period and for all the variables. ITS provides a single metric to identify the months that are closest to the mean of each variable under study and that are also temporally stable (Zhao *et al.*, 2010; Zhang *et al.*, 2022). The point with the most representative conditions of the whole dataset is identified as the one with the lowest ITS (closest to zero), and threshold values of the ITS can be used to identify the most divergent months (López-Vicente *et al.*, 2023). Finally, considering the different periods obtained in the breakpoint analysis, the MRD parameter of each variable was calculated again for each period, and the results were evaluated in the context of the climate change that already occurred between 1934-2023. The comparative analysis was carried out with parametric (ANOVA) and nonparametric (Kruskall Wallis) tests according to the normality of the data.

2.3.3. Influence of ENSO

The behaviour of the ENSO phenomenon was evaluated through the Oceanic Niño Index (ONI). It is NOAA's primary index for tracking the ocean part of ENSO, and it has become the de facto standard that is used for classifying El Niño and La Niña events in the eastern tropical Pacific. The monthly sea surface temperatures (STT) for the Niño 3.4 region were obtained at NOAA (2024) and the average monthly temperature was calculated for the 1934-2023 period. The difference from the average (anomaly) of each month of the study period was subsequently calculated. The ONI index was finally expressed as the rolling 3-month average temperature anomaly. Periods with different means and/or variances were searched for, using the same statistical packages cited in section 2.3.1, for the annual ONI values (calculated by averaging the quarterly values).

In addition, frequency analysis of ONI values (according to the quarterly timeframe scale of three months reported by NOAA) between those periods was performed via the Chi-square test. The ONI values were classified according to NOAA: neutral (-0.5 to +0.5), El Niño (above +0.5) and La Niña (below -0.5). The threshold was further broken down into Weak (with a +- 0.5 to +-0.9), Moderate (+- 1 to +-1.4), Strong (+- 1.5 to +-1.9) and Very Strong (≥ +- 2) events.

To determine the possible effect of the ENSO phenomenon on precipitation variables (teleconnection), linear correlations were established between the ONI and the four calculated rainfall variables. All of them were calculated quarterly (according to the same ONI time cut-off). Correlations were made between the same quarters and between outdated quarters (up to 2 quarters later), considering possible delays in response time for the region (Camilloni, 2006; Jozami *et al.*, 2015).

A schematic summary of the work conducted for each of the specific objectives of the study is presented below (Fig. 2.), considering the available data, the analyses performed, and the variables under study.

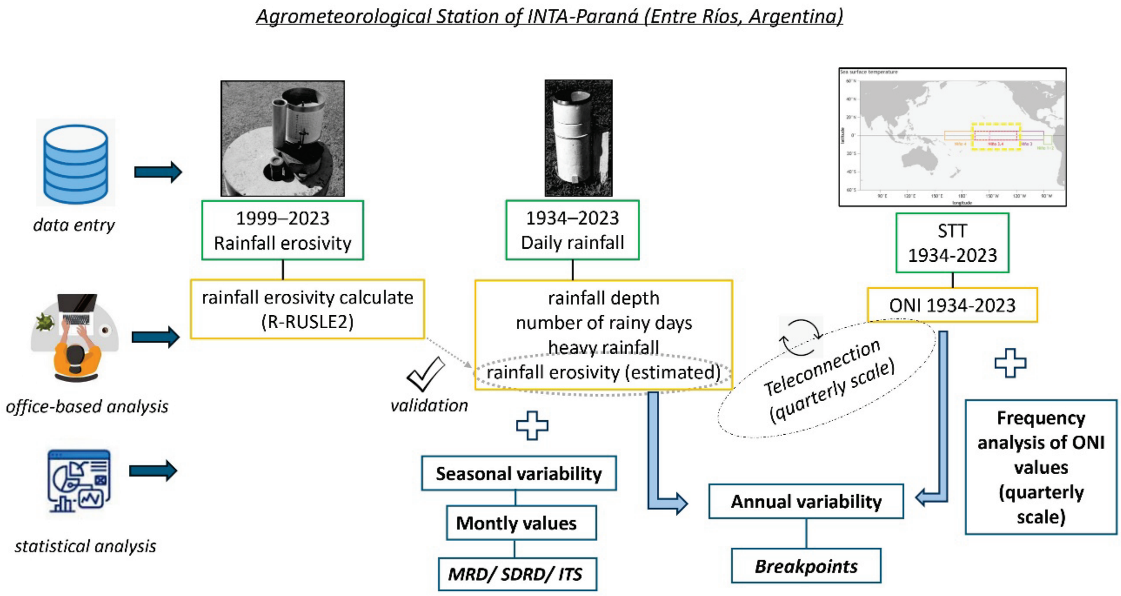

Figure 2. Conceptual framework illustrating the workflow and variables considered in this study.

3. Results

3.1. Evolution of rainfall depth, rainy days and heavy rainfall between 1934-2023

Average annual rainfall for the 90 years was 1029 mm, with the two highest values registered in the second half of the data series (1818 mm in 1978, and 1617 mm in 2000), and the two lowest values obtained in the first half of the data series (494 mm in 1937, and 532 mm in 1962). The annual rainfall depth exhibited marked interannual variability, with a median and standard deviation values of 1021 and 239 mm, respectively. Rainfall showed a spring–summer–autumn concentration, with the highest records in March (14.8%) and the lowest in July (2.8%) (Fig. 3a). Average annual number of rainy days was 76 days, with a maximum value of 114 days (year 2001) and a minimum of 39 days (year 1935). The median and standard deviation were 78 and 14 days, respectively. Despite the monthly distribution of rainy days did not show the marked differences of rainfall depth, a decrease in the magnitude of both variables occurred during winter season (Fig. 3b). Concerning heavy rainfall (percentage of precipitation on days with ≥ 50 mm concerning total precipitation), the average annual value was 28.2%, with a maximum value of 49.7% obtained in 2023 and a minimum value of 0% found in 1937, 1962 and 1968. Heavy rainfall in the winter months presented the lowest percentages (following the precipitation regime of the area) (Fig. 3c). The median and standard deviation were 28.7% and 12.2%, respectively.

Analyses to identify breakpoints in all four series revealed two periods with different means, with the breakpoint always occurring in the decade of 1970s. Annual rainfall breakpoint was in 1975 (p-value = 0.0022). The average precipitation in the second period (1100 mm) was 16% greater than that in the previous period (Fig. 4a). For the annual number of rainy days, the breakpoint year was 1972 (p-value = 1.95E-06), with a means of 69 and 82 days (19% greater) in the first and second periods, respectively (Fig. 4b). In terms of heavy rainfall, the breakpoint was in 1971 (p value= 0.03365). During the second period, there was a 21% increase in the percentage of heavy rainfall, with mean values of 25.2% and 30.5% in periods I and II, respectively (Fig. 4c).

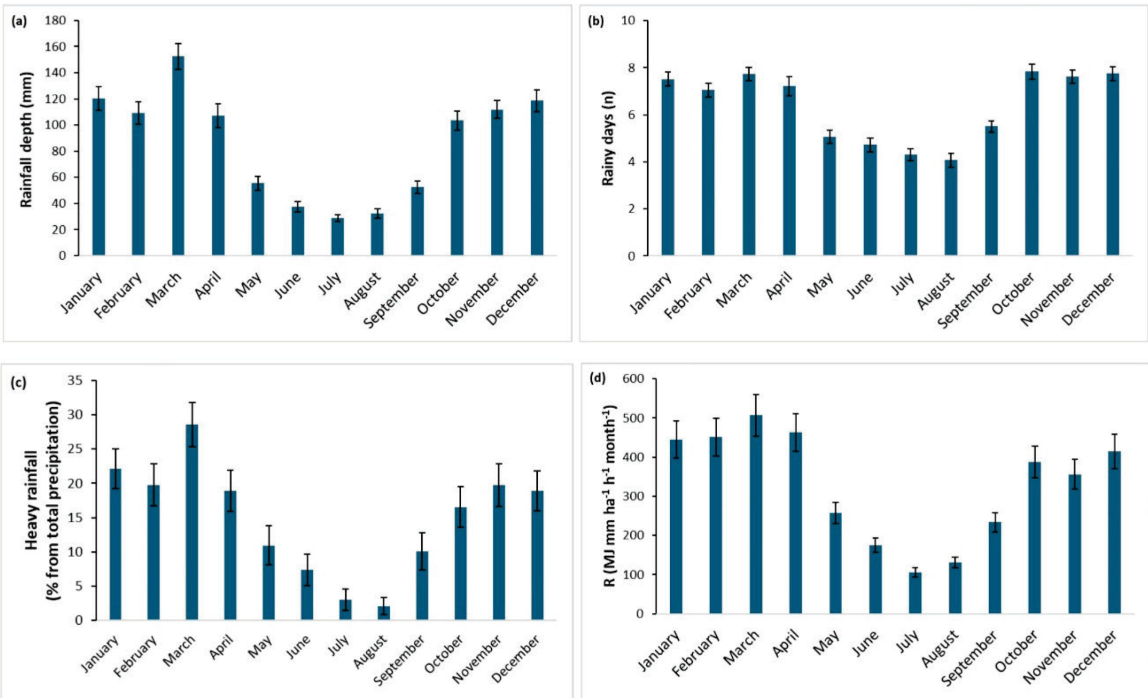

Figure 3. Monthly mean rainfall depth (a), number of rainy days (b), heavy rainfall (c), and rainfall erosivity –linear approach– (d) calculated for the period 1934-2023. Vertical lines represent standard error of the mean (SEM).

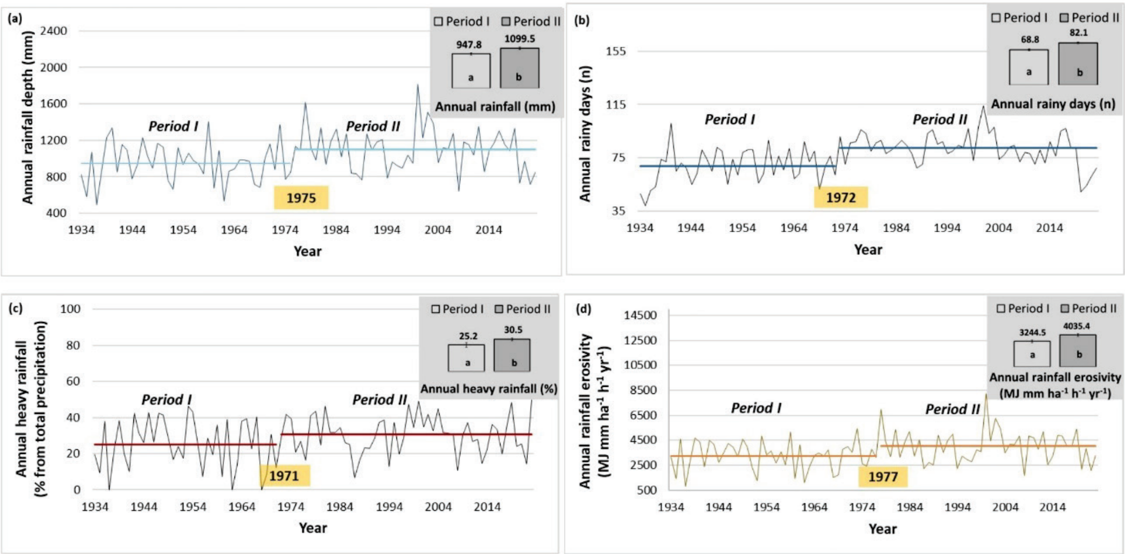

Figure 4. Annual values (1934-2023) and mean and standard errors (inset figure) in periods I and II according to breakpoint (breakdate in an orange-filled box): annual rainfall (a); annual number of rainy days (b); annual heavy rainfall (%) (c); annual rainfall erosivity (d). Inset figures: different letters indicate significant differences between the periods (ANOVA test LSD Fisher, p < 0,05) and vertical lines represent standard error of the mean (SEM).

3.2. Evolution of rainfall erosivity based on annual data between 1934-2023

3.2.1. Robustness of the linear approach of rainfall erosivity

For the period from 1999-2023, with larger time-resolution data, the average annual values of R were 4194 and 8311 MJ mm ha^{-1} h^{-1} yr^{-1} according to the approach of de Santos Loureiro and de Azevedo Coutinho, and RUSLE2 equations, respectively. The correlation coefficient (Spearman) for the annual values was 0.80 (n=25) (Supplementary content 1a), and for the monthly values was r=0.87 (n=300) (Supplementary content 1b).

3.2.2. Rainfall erosivity trend

The average annual rainfall erosivity (R) for the whole period (1934-2023) was 3649 MJ mm ha^{-1} h^{-1} yr^{-1} and the years with the maximum (8222 and 6939 MJ mm ha^{-1} h^{-1} yr^{-1}) and minimum (797 and 1086 MJ mm ha^{-1} h^{-1} yr^{-1}) rainfall erosivity were the same as those of the annual rainfall. The distribution of rainfall erosivity over the months mirrored the behaviour of the rainfall depth (Fig. 3d). The breakpoint of R appeared in 1977 (p-value = 0.0032). The erosivity value during the second period was 24% greater than that during the first period: 4035 and 3244 MJ mm ha^{-1} h^{-1} yr^{-1}, respectively (Fig. 4d). As for the previous variables, rainfall erosivity showed a marked interannual variability, with a median and standard deviation of 3603 and 1293 MJ mm ha^{-1} h^{-1} yr^{-1}, respectively.

3.3. Correlation of the parameters

The linear correlations between the four precipitation variables at the annual scale were significant in all the cases (Table 1), with coefficients ranging from 0.96 (between rainfall depth and rainfall erosivity) to 0.23 (heavy rainfall and rainy days). The significant influence of 'heavy rainfall' on rainfall erosivity is noteworthy, with a coefficient even higher than that obtained with the variable 'rainy days' (r= 0.70 vs 0.52).

*Table 1. Pearson's coefficients of the rainfall variables at the annual scale (n=90) (**p-value<0,0001, *p-value<0.05).*

	Rainfall depth	Rainy days	Heavy rainfall	Rainfall erosivity
Rainfall depth	1			
Rainy days	0.67**	1		
Heavy rainfall	0.58**	0.23*	1	
Rainfall erosivity	0.96**	0.52**	0.7**	1

3.4. Seasonal variability

3.4.1. Analyses of variables on a monthly scale (1934-2023)

The monthly variability of rainfall yielded the following points (Fig. 5a): I) The months of the period from May-September were those that, on average (T=90 years), had negative MRD values (below monthly average rainfall). Specifically, the winter months (June, July, August) were 60% drier than the monthly average, and this behaviour was moderately stable (which means that it was a behaviour with some confidence of occurrence). The remaining months had positive MRD values (moister conditions). The analysis of the distribution of the data (quartiles) allowed classification into dry months: July and August (values < to Q1: 37.3 mm); and wet months: December, January and March (values > to Q3: 111.7 mm). June and November were on the border lines of Q1 and Q3, respectively. And II) Regarding the temporal stability (ITS) of the monthly values, December, January and March were the most unstable in the period analysed, and thus, their behaviour was less predictable.

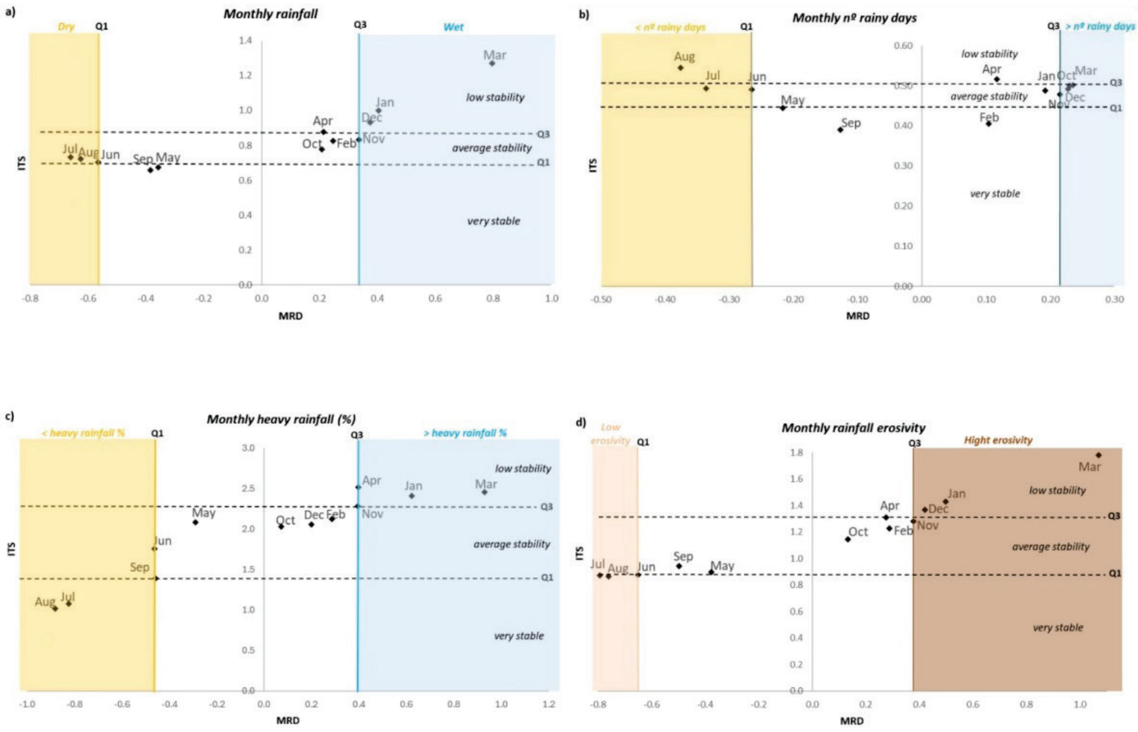

Figure 5. Monthly values of the mean relative difference (MRD) and index of temporal stability (ITS) of rainfall depth (a); number of rainy days (b); heavy rainfall (c); and rainfall erosivity (d) for the 90-year study period (1934-2023).

The time series analysis of the monthly number of rainy days (Fig. 5b) revealed greater stability than the rainfall depth did. Compared with those of monthly rainfall, MRD values presented smaller differences between months and lower values of ITS. However, some differential behaviours of certain months could be highlighted. Although high monthly rainfall values did not occur in October, it presented a high number of rainy days. In contrast, January, despite its high monthly rainfall values, did not have high values of rainy days. Finally, it should be noted that for this variable, the winter months show the same or greater instability than the summer months do: August had the highest value of ITS for this variable, despite its stability in the values of rainfall depth.

In terms of monthly heavy rainfall (Fig. 5c), there was a higher difference between months, as shown by the range of MRD values, and also higher instability values (ITS). March and January were the months with the highest values. December presented values in an 'intermediate' range (despite its high MRD values for rainfall depth and rainy days). With respect to the temporal stability, the high value of the ITS in April stood out as the most unstable month for this variable, followed by January and March.

The analysis of monthly rainfall erosivity is summarized in Fig. 5d, which shows that it followed the same behaviour as the variable monthly rainfall, as expected, although with greater temporal instability in general. The monthly ITS values for this variable were exceeded by 'heavy rainfall', which shows the greatest instability in its monthly pattern (Supplementary content 2). The joint analysis of the variables, revealed that December, January, and especially March, were the most erosive months, which was also related to their high monthly rainfall values. In addition, March and January had the highest values for the variable heavy rainfall, which was considered an important factor for its potential impact on erosivity. March stood out concerning its instability during the whole period for the four variables. Within the summer months, the values of February differ from the other months, with low values for the variables analysed and greater stability. Finally, it should be noted that, in general, the winter months are more stable, except for 'rainy days', where the ITS values are equal to or greater than those of the other months.

3.4.2. Monthly changes according to breakpoints

Considering the two periods defined in sections 3.1 and 3.2.2 –breakpoints–, the evolution of the MRD metric between the two periods was analysed at the monthly scale for each variable. In terms of monthly rainfall, significant differences were found in March and December. March decreased its value, i.e., in the second period it contributed to a lesser extent to annual rainfall: its lower MRD value implies a smaller difference from the average monthly rainfall value. However, in absolute values, it remains the wettest month, i.e., the one with the highest MRD value. The opposite occurred in December (Fig. 6). With respect to rainy days, a greater number of months showed variations between the periods. February and May increased, whereas March, June and September decreased (Fig. 7). The months of January and June presented decreases in heavy rainfall MRD values. Notably, for this variable, the high interannual variability and the presence of very high values made it difficult to detect significant changes. However, an increasing trend (nonsignificant) was observed for March and December (Fig. 8). For rainfall erosivity, a significant decrease was found only in March (Fig. 9).

Considering all variables and periods I and II (regardless of those months where a significant change could be detected), some trends of change were distinguished concerning the monthly patterns. A decrease in the monthly contribution for most of the variables (except for rainy days, which showed no variations) was highlighted for January, and the opposite occurred in December. For February and April, a trend toward higher values was observed for all the variables (except for heavy rainfall). The month of March presented particularities, given that although its contribution to monthly rainfall, rainy days and rainfall erosivity decreased, it tended to concentrate rainfall on days with more than 50 mm. This fact was important when considering the possible impacts of this tendency to increase intense rainfall and considering that it was the month with the highest absolute values for all variables. Finally, with a less marked upwards trend, a possible change in monthly behaviour was observed for May (with increases in MRD values).

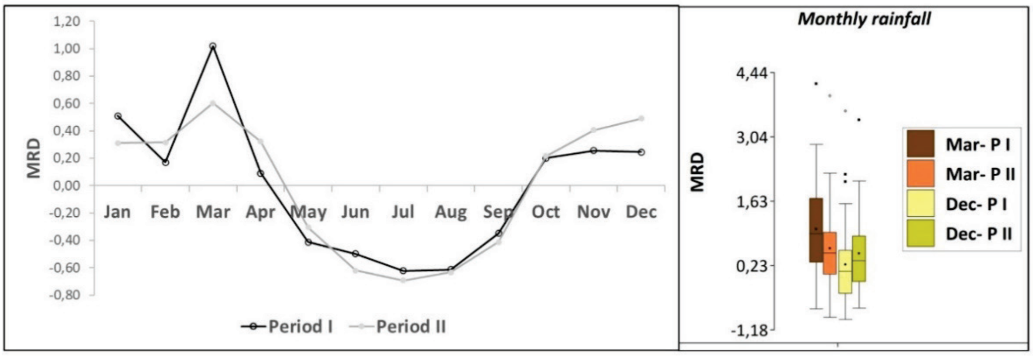

Figure 6. Mean relative difference (MRD) values of monthly rainfall in periods I and II according to the breakpoint. Period I (P I: 1934-1975), Period II (P II: 1976-2023). The asterisks indicate significant differences between the MRD values of monthly rainfall for the periods at 0.10 (*) and 0.05 (**) (Kruskall Wallis test). On the right side: box plots for those months with significant differences.

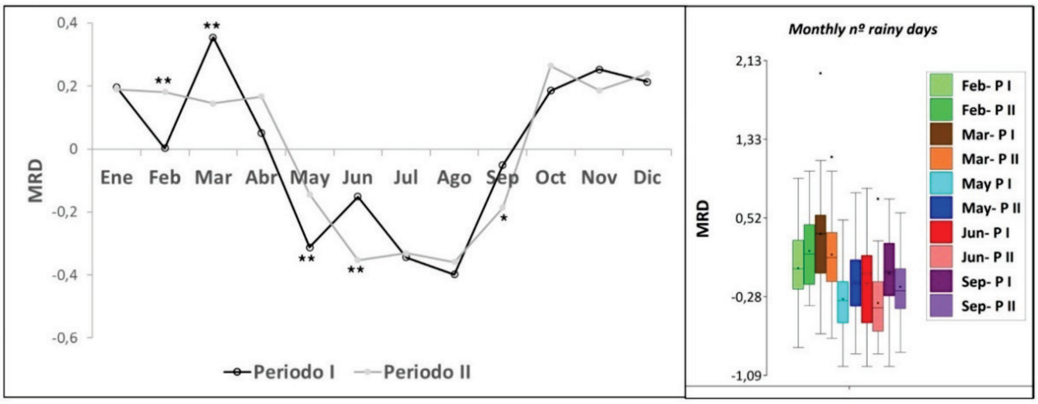

Figure 7. Mean relative difference (MRD) values of monthly number of rainy days in periods I and II according to breakpoints. Period I (P I: 1934-1972), Period II (P II: 1973-2023). The asterisks indicate significant differences between the MRD values of number of rainy days for the periods at 0.10 (*) and 0.05 (**) (ANOVA). On the right side: box plots for those months with significant differences.

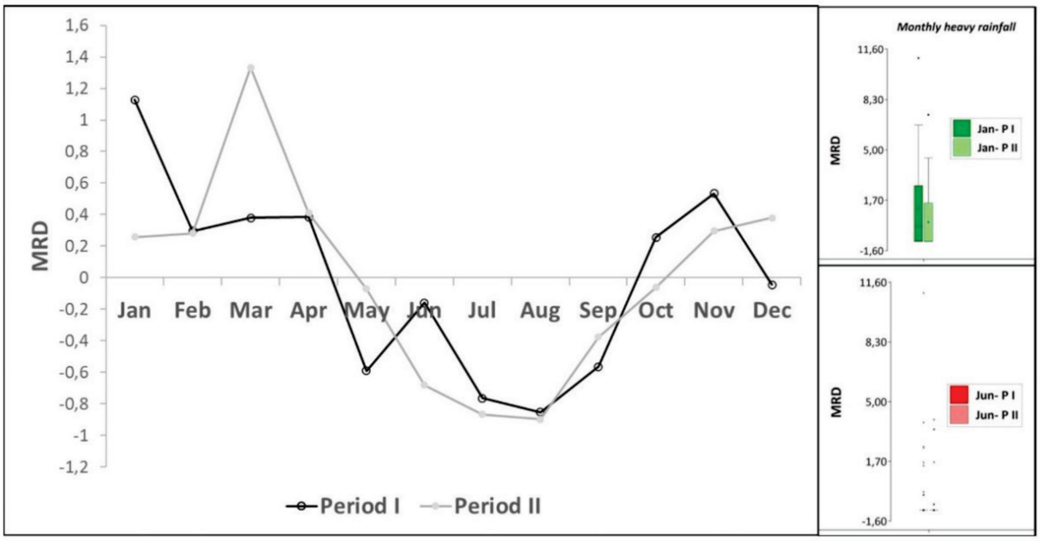

Figure 8. Mean relative difference (MRD) values of monthly heavy rainfall in periods I and II according to breakpoints. Period I (P I: 1934-1971), Period II (P II: 1972-2023). The asterisks indicate significant differences between the MRD values of heavy rainfall for the periods at 0.10 (*) (Kruskall Wallis test). On the right side: box plots for those months with significant differences.

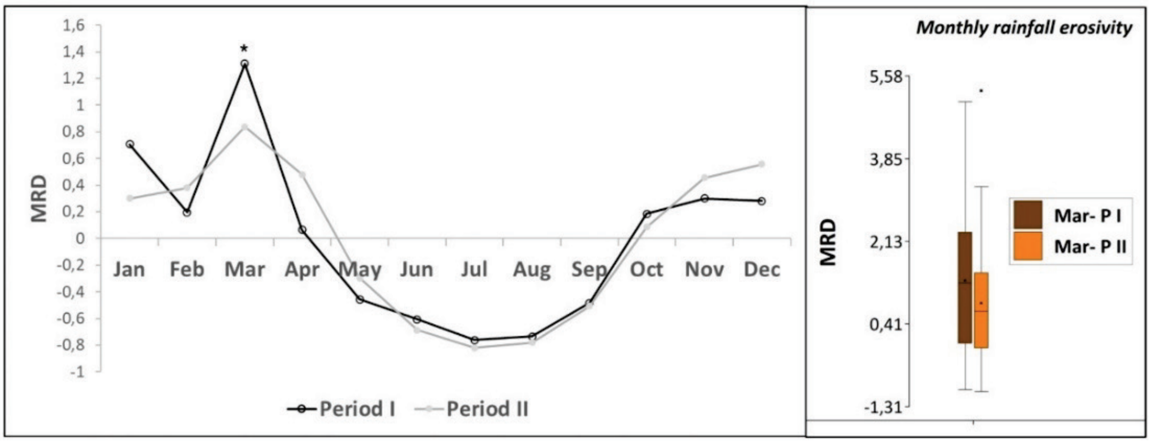

Figure 9. Mean relative difference (MRD) values of monthly rainfall erosivity in periods I and II according to breakpoints. Period I (P I: 1934-1977), Period II (P II: 1978-2023). The asterisks indicate significant differences between the MRD values of rainfall erosivity for the periods at 0.10 (*) (Kruskall Wallis test). On the right side: box plots for those months with significant differences.

3.5. Rainfall parameters and El Niño/Southern Oscillation (ENSO)

The analysis to detect periods with differences in the mean and/or variance on ONI annual values detected a breakpoint in 1975. The first period presented a mean annual ONI value of -0.11, whereas the second period presented a mean annual ONI value of 0.09 (p value=0.10) (Supplementary content 3). The analysis to determine changes in the frequencies of these anomalies was performed taking into account this breakpoint on the basis of the evolution of the ONI quarterly index. The results revealed differences between the frequencies for the two periods (Chi2 test, p= 0.0002). In general, an increase in the frequency of all the ranges of "Niño" stands out (Fig. 10). The frequency of negative anomalies (ONI values < -0.5) was 139 *vs.* 134, whereas that of positive anomalies (ONI values > 0.5) was 83 *vs.* 159 (periods I and II, respectively). Notably, there was a marked increase in the number of strong Niño events (from 1.2% to 3.8%) and very strong Niño events (from 0.2% to 2.8%) in the second and recent periods (1976-2023) with respect to the first and oldest periods (1934-1975).

Significant positive correlations were found between some of the quarters analysed for the ONI Index and the estimated variables of precipitation (Table 2). In general, the quarters covering the spring and summer seasons presented significant relationships, with higher values than those obtained for the summer. In particular, the highest correlations were found for the variables rainfall depth and erosivity for the quarters November/December/January (NDJ) and December/January/February (DJF), considering both the correlation with the ONI for the same quarter and with previous quarters (teleconnection). Finally, it should be noted that those correlations that presented higher values when considering effects in subsequent months on the rainfall parameters occurred mainly for the ONI values from the July/August/September (JAS) to October/November/December (OND) quarters, with effects on the rainfall parameters assessed in the spring-summer months. The variable heavy rainfall, presented the lowest correlation values, although it should be noted that the teleconnection was more present in the ONI values of the spring-summer quarters. Finally, there were quarters of the ONI without any correlation with the assessed rainfall parameters: February/March/April (FMA), March/April/May (MAM) and June/July/August (JJA).

Figure 10. Frequency of ONI quarterly values according to periods of analysis: 1934-1975/1976-2023. Inset figure: Evolution of the quarterly ONI Index (1934-2023). The lines show values above the neutral threshold ±0.5.

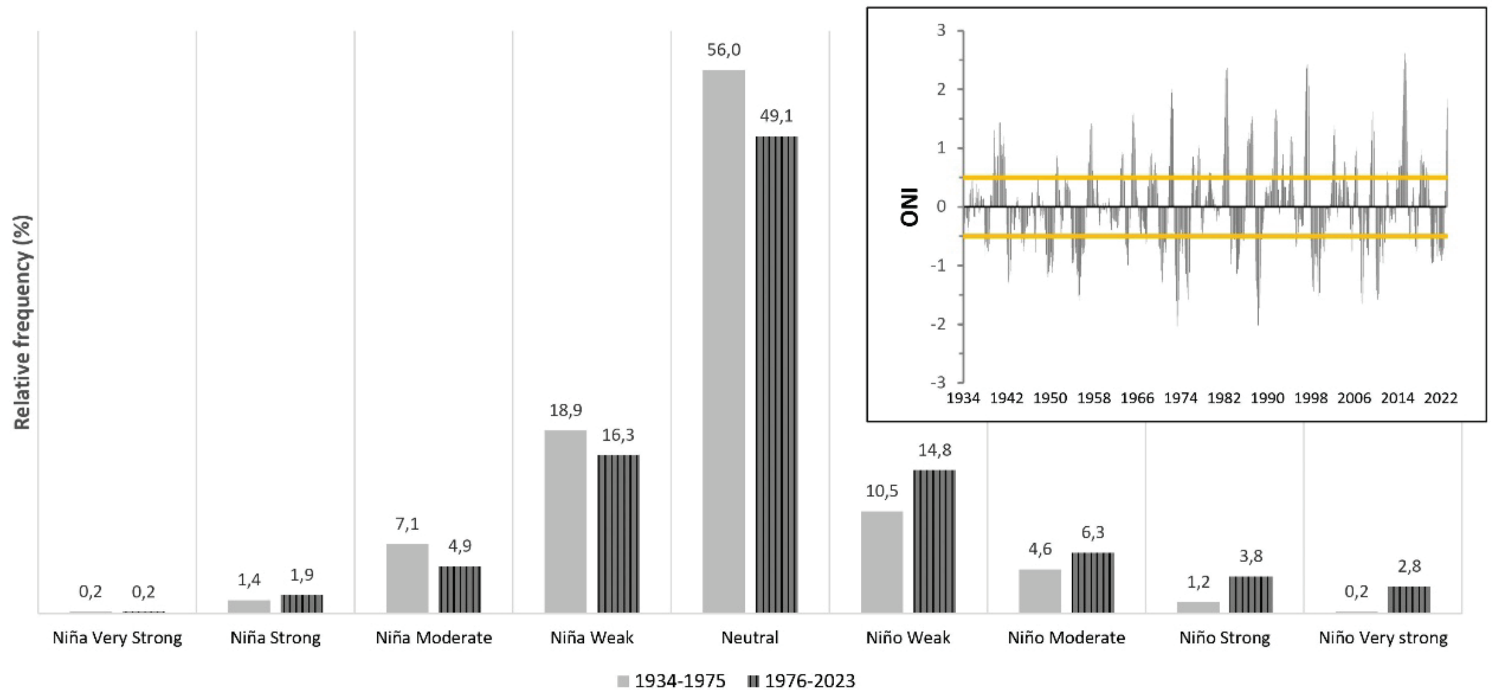

*Table 2. Pearson correlation between the variables according to quarters set by the ONI index (n=90). The underlined values represent correlations between lagged quarters with higher values than their same quarter. The gray-colored cells indicate ONI quarters without any correlation with the rainfall parameters. December/January/February (DJF), January/February/March (JFM), February/March/April (FMA), March/April/May (MAM), April/May/June (AMJ), May/June/July (MJJ), June/July/August (JJA), July/August/September (JAS), August/September/October (ASO), September/October/November (SON), October/November/December (OND), November/December/January (NDJ), and Oceanic Niño Index (ONI) values (***p value<0,0001, **p value<0.05).*

Pearson's Correlation		Rainfall depth						Rainfall erosivity						Rainy days						Heavy rainfall			
		DJF	JFM	FMA	SON	OND	NDJ	DJF	JFM	FMA	SON	OND	NDJ	DJF	JFM	FMA	MAM	OND	NDJ	DJF	JFM	MJJ	NDJ
ONI	DJF	0.46 ***	0.31 **	0.24 **				0.45 ***	0.33 **	0.21 **				0.27 **		0.22 **				0.28 **	0.29 **		
	JFM		0.27 **						0.28 **								0.22 **				0.28 **		
	FMA																						
	MAM																						
	AMJ																					0.22 **	
	MJJ																					0.28 **	
	JJA																						
	JAS				0.26 **						0.23 **												
	ASO				0.25 **	0.44 ***					0.23 **	0.36 **						0.32 **					
	SON				0.26 **	0.44 ***	0.5 ***				0.23 **	0.36 **	0.45 ***					0.32 **	0.39 **				0.22 **
	OND	0.46 ***				0.43 ***	0.5 ***	0.45 ***				0.35 **	0.45 ***	0.3 **				0.3 **	0.38 **	0.25 **			
	NDJ	0.47 ***	0.33 **				0.51 ***	0.46 ***	0.35 **				0.46 ***	0.3 **					0.38 **	0.26 **	0.29 **		0.22 **

4. Discussion

4.1. Rainfall parameter evolution

The number of studies that analyse and discuss changes in climate has increased considerably in recent years, although many issues need further investigation, particularly for developing countries (Penalba and Bettolli, 2011). The results of this study agreed with reports in the literature at different scales: the global (Intergovernmental Panel on Climate Change, 2023, Alexander *et al.*, 2006), regional (Magrin *et al.*, 2014a, Re and Barros, 2009), national (Magrin *et al.*, 2014b, Podestá *et al.*, 2009) and even local (Wingeyer *et al.* 2022) scales.

In particular, many studies focused on Argentina have evaluated rainfall, and some have analysed it through the search for breakpoints. For the northwestern region of Argentina (28°S--38°S, 65°W--70°W), Compagnucci *et al.* (2002) reported a 20% increase in the mean summer precipitation, with a breakpoint detected in 1977. In general, the available studies highlighted the high interannual variability presented in the data series, which usually did not allow for assuring trends with probabilities greater than 90%. However, Barros *et al.* (2015) reported an increase in precipitation over most subtropical Argentina in late 1960, with some trends of over 5 mm yr^{-1}. In our study, the difference in rainfall depth between the two periods was 152 mm, equivalent to 3.16 mm yr^{-1} from 1976 to the present (95% confidence interval). Penalba and Vargas (2004) stated that there was nonstationary variability in central-northeastern Argentina, with increases in annual precipitation from 1950 onwards. For the eastern part of the country (including the study area of this study), they noted that there was an increasing trend and not a jump or breakpoint (which was observed in the west of the country). They analysed the influence of this trend on the extreme precipitation (negative and positive) of the years/months from 1901-2000. The authors stated that there was an influence with periods with greater deficits and surpluses, although they stated that in the last 30 years of the time series, there was a consistent increase with surpluses with respect to the average annual precipitation.

In addition to identifying two periods with different means for annual rainfall (defined by a breakpoint in the 1970s), this study identified another breakpoint within the same decade for the variable heavy rainfall. This result revealed that, concerning total annual rainfall, there was an increase in the number of millimetres fallen on days with more than 50 mm. This variable is particularly relevant because of its potential impacts on the urban and rural environments. A recent study analysed this variable in Europe because of its importance in increasing flooding. In conclusion, the increasing trend in flood extent over central Europe can be attributed to an increase in the spatial extent of heavy precipitation (Fang *et al.*, 2024). For Argentina, a positive trend in the frequency of heavy rainfall events over thresholds ranging from 50 to 150 mm has been detected since 1960, especially in central and eastern between 30°S and 40°S (Barros *et al.*, 2015). However, no studies have analysed this variable as the percentage of rainfall on days with more than 50 mm with respect to the monthly and annual total rainfall. Even less so for years prior to the 1950s or 1960s, the results presented here are considered to contribute to the scientific literature on this topic.

With respect to rainfall erosivity, the fit in the correlation found between the estimation concerning the calculation of rainfall erosivity obtained through the RUSLE2 formula is considered appropriate, similar to the results in Portugal reported by de Santos Loureiro and de Azevedo Coutinho (2001). Due to the limited availability of high-resolution historical data required for the calculation of R-RUSLE2, the validation of this fit was conducted using a recent time series. Nevertheless, future studies should assess the applicability of this approach using longer-term datasets in regions with similar rainfall regimes, where precipitation data at 15- or 30-minutes temporal resolution are available. Moreover, the annual values of R (according to the linear equations) for the periods 1999-2023 (4194 MJ mm ha^{-1} h^{-1} yr^{-1}) and 1934-2023 (3649 MJ mm ha^{-1} h^{-1} yr^{-1}) are comparable to, although higher than, the estimated values for all of Argentina in the recent study by Panagos *et al.* (2017) (2232 MJ mm ha^{-1} h^{-1} yr^{-1}). This difference is reasonable because of the different climates and regions present throughout the country.

The observed increase in rainfall erosivity was in line with that reported by Casas (2015) for Argentina. For Northeast Argentina, Saluso (2008) estimates values approximately 10--15% higher between 1950--1994 and 1995--2005. Additionally, Crettaz *et al.* (2016) find more marked increases when the values are updated up to 2014, with increases of more than 20% for the Department of Paraná (Entre Ríos). The percentage increase in this variable between the two periods was similar to the global projections for 2050 and 2070 calculated by Panagos *et al.* (2022).

With respect to the analysis on a monthly scale, no previous work has been reported that calculates the monthly patterns (MRDs) of different precipitation variables for a series of 90 years and, above all, analyses the temporal stability (ITS) of these patterns. In general, the winter months presented values below the monthly averages and a more stable pattern with respect to the other months. Except for the variable 'rainy days', where its instability was high. The variable with the most unstable monthly pattern was 'heavy rainfall', followed by 'rainfall erosivity', 'rainfall depth' and 'rainy days'. The comparison between periods according to their breakpoint year allowed us to see some trends of change in the monthly patterns, despite the high interannual variability.

The influence of ENSO phases on precipitation has been widely studied, leading to the conclusion that rainfall in several regions throughout the world is influenced by the equatorial Pacific SST and its associated anomaly circulations (Re and Barros, 2009). One of these regions is southeastern South America, and many studies have shown that it has a greater or lesser influence on the study area. Forgioni *et al.* (2023) analysed its relationship (based on ONI values) with respect to the precipitation during the summer months (November–December–January quarter) in the province of Santa Fe, which is located west of the province of Entre Ríos. This period was chosen because of its importance as a critical period for the most important summer crops in the Argentine Pampas region (corn, soybeans, sunflower, sorghum). They highlighted the high spatiotemporal variability of the correlation, although the analysis generally revealed an increase in correlations between 1971 and 2020. Barros *et al.* (2015) reported that for the north of the country, half or more of the positive annual rainfall trend occurred during the El Niño phase. However, in the rest of subtropical Argentina, especially south of 30°S, increased precipitation (in the early 1960s) occurred mostly during months of the neutral phase of the El Niño/Southern Oscillation (ENSO), with only small trends during the months of El Niño and La Niña. Another study in the Pampean region reported correlations between the ONI and rainfall erosivity (from 2001 to 2013), with a coefficient of 0.59 on an annual scale (Behrends Kraemer *et al.*, 2018). Finally, a recent paper (N. Di Leo *et al.*, 2024) analyses temporal and spatial variability in the Pampean region, considering ONI and summer precipitation (NDJ quarter). For Entre Ríos they detected positive and high correlations during the whole period (1990-2021). However, for the region as a whole, they observed high temporal and spatial variability, suggesting the existence of influences from other climatic factors. In the present study, the increase in the rainfall variables analysed was detected in the 1970s, and significant correlations were found (with coefficients not exceeding 0.5) for the behaviour of ENSO (through the ONI index) and its effect on rainfall depth and erosivity, especially considering the spring–summer months. Finally, at this point, a change in the behaviour of the ONI was detected through the search for breakpoints in the time series, which coincided with the breakpoint year of annual precipitation. However, an increase in the frequency of extreme positive values of the ONI after 1976 (Period II) was detected, which could be related to the increase in rainfall variables observed from the 1970s onwards.

Future scenarios estimate that the general precipitation increase experienced over the last 50 years for eastern and central subtropical Argentina would not be reversed during the rest of this century and that the observed positive trends in extreme monthly precipitation since 1960 are projected to continue (Barros *et al.*, 2015). However, a recent global study, which considered different models, projected an erosivity increase of 12.9% in 2050 and a reduction to 11.5% in 2070 for South America (Panagos *et al.*, 2022).

In this framework, and considering the findings for the study area, it is considered relevant to be able to anticipate the effects of both an increase and a decrease in rainfall (according to the months of interest), as well as the consequences of increases or decreases in rainfall erosivity and the occurrence of heavy rains on the environments and productive activities that take place there.

4.2. Agronomic relevance of the results

Climate variability, particularly extreme climate anomalies, has a negative impact on regions where the economy is based on agriculture, such as the Pampas, which comprises the most productive agricultural lands of Argentina (Penalba and Bettolli, 2011). The largest amount of grains (soybean, corn, wheat, sunflower) and other crops are grown in this region and constitute one of the principal sources of fiscal income. Although the country has a diversified industry, agriculture and its direct manufactures add up to 55% of the export revenue (Barros *et al.*, 2015). As most of it is produced without irrigation, precipitation is one of the climatic variables with the main influence on production.

The province of Entre Rios has a strong agricultural sector: in the 2022/2023 campaign it accounted for 6.3% of the total area sown at the national level. The main crops were soybean, wheat and maize, which together accounted for 88.5% of the area sown and 82.8% of production at the provincial level. Within the province of Entre Ríos, the Department of Paraná concentrates important percentages of soybean, sorghum, wheat, sunflower and corn production (Informe del sector Agrícola Provincia de Entre Ríos, 2023). The observed seasonality of rainfall favours the production of summer crops, and the tendency towards an increase in December –with statistical significance– and in a minor way in November and February could further increase this situation. However, the high variability and increase in extreme events (e.g., due to an increase in the frequency of Strong Niño events) could harm the sector. Despite these results, in the last years of the time series analysed (campaign 2022/2023) there were negative results for all production parameters as a result of adverse weather conditions and severe drought (La Niña phenomenon), which affected mainly summer crops (maize, soybean, sorghum and rice) and also the production of fodder for livestock (Government of Entre Ríos, 2019). The ability to plan and prepare for these extreme weather event scenarios is essential.

The negative effects of these events may also occur if we consider the soil erosion processes caused by increased erosive rainfall, which requires attention to the different monthly behaviours. The month of March stood out for its important contribution to the annual values of all the parameters (reflected in its high MRD values), but at the same time, it showed high instability. In the case of monthly rainfall, rainy days and rainfall erosivity, this could be related to the decreasing trend over the last 50 years for this month. However, the concentration of rainfall on days with more than 50 mm, the most erosive events, showed a positive trend. This situation occurs in March, and considering that summer crops no longer have a considerable water demand at this time of year, they could have negative effects. Proposals such as interplanting cover crops before harvesting would allow the use of available water and an improvement in cover with positive impacts on the reduction in soil erosion. Another special attention deserves the month of May, which significantly increased the number of rainy days in the last 50 years and had an increasing trend (although not significant) for the remaining variables. During this month, in many agricultural areas of Entre Ríos, the soil is without crops planted, which would require specific practices to mitigate soil erosion. This is also important if we consider a scenario with a possible increase in intense rainfall and approximately 70% of the land surface of Entre Ríos with soils with vertic characteristics (Vertisols and associated vertic Mollisols and Alfisols) and low infiltration capacity (Sasal *et al.*, 2019). Furthermore, it is recommended to consider possible modifications to the calculations made for soil erosion, taking into account these possible increases in erosivity and/or rainfall intensity.

Penalba and Bettolli (2011) highlighted the importance of diagnosis and forecasting, particularly in the context of future climate change. The results of their analyses based on different climate models imply an increase in the variability of daily rainfall, especially during summer, and a change in the distribution of rainfall over the Pampas region. They argued that while favourable consequences for agricultural production trends could be estimated for increased precipitation (and a context of climate change with higher temperatures), there was significant intermodel scatter and uncertainty in the understanding of extreme events and in the ability of models to represent their occurrence. Similarly, Barros *et al.* (2015) argued that the risks associated with more frequent extreme weather events are increasing, even though climate change in recent decades has favoured agricultural productivity in many areas. While increased rainfall and temperatures could improve productivity, their impact on evapotranspiration and increased pests is unknown.

5. Conclusion

This study, which was carried out for a locality in the Pampean region of Argentina with characteristics that make it susceptible to water erosion, presents interesting findings regarding changes in the rainfall parameters analysed. Taking a long period of study (90 years) and daily data, significant increases in rainfall, number of rainy days, percentage of rainfall on days with more than 50 mm and rainfall erosivity (estimated) since the 1970s were evident. For the first time, this study has calculated the values and temporal evolution of heavy rainfall and rainfall erosivity in the decades of the 1930s, 1940s and 1950s, both at annual and monthly scales, incorporating these results for a better comprehension of the effects that climate change had on precipitation variables. Special attention is recommended for the months of March, January and December, given that in the 90 years of the study, these months presented the greatest instability in their temporal pattern with respect to rainfall and erosivity, as well as being the wettest and most erosive. In addition, future work will further analyse the possible changes detected at the monthly level in this paper. Our results were consistent with a change in the mean values of the ONI related to the El Niño–Southern Oscillation phenomenon. The latter is associated with an increase in the frequency of positive outliers (related to wetter periods) and with significant correlations with selected rainfall parameters. This finding, and even more so if we take into account some climate change models that estimate increases in extreme events (both wet and dry periods), highlights the need to reinforce soil resource protection measures and agricultural practices that make better use of water as a function of possible changes in rainfall patterns.

Acknowledgements

This work was supported by INTA (through the Programa de Posgrado y Perfeccionamiento en el Exterior P176905–BIRF- RESOL-2023-342-APN- CD#INTA, to M.S. Seehaus). Support for the mobility and dissemination of research results was also provided through “Programa de Galicia FEDER 2021-27” and “Axudas do programa de consolidación e estruturación de Grupos de investigación competitivos (GRC)- Xunta de Galicia: AQUATERRA”.

We thank the members of the Agrometeorological Station of INTA-Paraná, who over the years have carried out a careful recording of meteorological variables. Additionally, the staff of the Departamento de Recursos Naturales y Gestión Ambiental for their valuable contribution in the reading of 25-year rainfall bands. Finally, we would like to thank Centro Interdisciplinar de Química e Bioloxía (CICA- Universidade da Coruña) for its contribution to the climate and erosivity analysis.

Author contribution

Mariela Soledad Seehaus: conceptualization, formal analysis, investigation and writing—original draft. Manuel López-Vicente: conceptualization, formal analysis, and writing—original draft. Ana Beatriz Wingeyer: conceptualization, formal analysis, investigation, writing – review and editing.

Maria Carolina Sasal: conceptualization, supervision, writing – review and editing. Alejandra Lorena Cuatrin: formal analysis. Emanuel Melgares: investigation.

References

Alexander, L.V., Zhang, X., Peterson, T.C., Caesar, J., Gleason, B., Klein Tank, A., Haylock, M., Collins, D., Trewin, B., Rahimzadeh, F., Tagipour, A., Rupa Kumar, K., Revadekar, J., Griffiths, G., Vincent, L., Stephenson, D.B., Burn, J., Aguilar, E., Brunet, M., Taylor, M., New, M., Zhai, P., Rusticucci, M., Vazquez-Aguirre, J.L. 2006. Global observed changes in daily climate extremes of temperature and precipitation. *J. Geophys. Res. Atmos*. 111, D05109. https://doi.org/10.1029/2005JD006290

Almagro, A., Oliveira, P.T.S., Nearing, M.A., Hagemann, S. 2017. Projected climate change impacts in rainfall erosivity over Brazil. *Sci. Rep.* 7, 8130. https://doi.org/10.1038/s41598-017-08298-y

Angulo-Martínez, M., López-Vicente, M., Vicente-Serrano, S.M., Beguería, S. 2009. Mapping rainfall erosivity at a regional scale: A comparison of interpolation methods in the Ebro Basin (NE Spain). *Hydrol. Earth Syst. Sci.* 13 (10), 1907-1920. https://doi.org/10.5194/hess-13-1907-2009

Ares, M.G., Varni, M., Entraigas, I. 2010. Determinación de la erosividad de las precipitaciones para la localidad de Azul, provincia de Buenos aires, Argentina, in Varni, M., Entraigas, I., Vives, L. (Eds.), *Hacia la Gestión Integral de los Recursos Hídricos en Zonas de Llanura*. Ed. Martin, Mar del Plata, Argentina. ISBN: 978-987-543392-2, pp. 95-99. http://hdl.handle.net/2133/7152

Bai J., Perron P. 1998. Estimating and Testing Linear Models with Multiple Structural Changes. *Econométrica* 66, 47-78. https://doi.org/10.2307/2998540

Barros, V., Castañeda, M.E., Doyle, M. 2000. Recent Precipitation Trends in Southern South America East of the Andes: An Indication of Climatic Variability, in Smolka, P., Volkheimer, W. (Eds.), *Southern Hemisphere Paleo- and Neoclimates*. Springer, Berlin, Heidelberg, pp 187-206. https://doi.org/10.1007/978-3-642-59694-0_13

Barros, V.R, Doyle, M., Camilloni, I. 2008. Precipitation trends in Southeastern South America: relationship with ENSO phases and the low-level circulation. *Theor Appl Climatol Theoretical* 93, 19-33. https://doi.org/10.1007/s00704-007-0329-x

Barros, V.R., Boninsegna, J.A., Camilloni, I.A., Chidiak, M., Magrín, G.O., Rusticucci, M. 2015. Climate change in Argentina: Trends, projections, impacts and adaptation. *WIREs Climate Change* 6(2), 151-169. https://doi.org/10.1002/wcc.316

Behrends Kraemer, F., Chagas, C., Ibañez, L., Carfagno, P., Vangeli, S. 2018. Análisis de la erosividad de las lluvias para el partido de San Pedro (BS. AS.). *Cienc. Suelo* (Argentina) 36 (1): 124-137. https://ri.conicet.gov.ar/handle/11336/105485

Bertocco, T., Figueiredo, T. de, Paz-González, A., García-Tomillo, A., López-Vicente, M. 2025. Deciphering sediment connectivity dynamic in traditional water-meadows (lameiros). *Geomorphology* 480, 109750. https://doi.org/10.1016/J.GEOMORPH.2025.109750

Camilloni, I. 2006. Short-term climate predictability of summer rainfall on the Paraná basin based on Atlantic and Pacific Sea Surface temperatures, in INPE (Ed.), *Proceedings of 8th International Conference on Southern Hemisphere Meteorology and Oceanography* (ICSHMO) (pp. 711-718).

Casas R.R. 2015. La erosión del suelo en la Argentina, in Casas R. R., Albarracín G. (Eds.), *El deterioro del suelo y del ambiente en la Argentina*. 1 ed., Vol. II. Centro para la Promoción de la Conservación del Suelo y del Agua, Fundación para la Educación, la Ciencia y la Cultura (FECIC). Ciudad autónoma de Buenos Aires, Buenos Aires, Argentina. ISBN 978-950-9149-39-7, pp. 433-452.

Crettaz, E., Gvozdenovich, J., Saluzzio, M. 2016. C*álculo del Factor R de la USLE a través del Índice Modificado de Fournier.* INTA Paraná. https://www.researchgate.net/publication/321058206_CALCULO_DEL_FACTOR_R_DE_LA_USLE_A_TRAVES_DEL_INDICE_MODIFICADO_DE_FOURNIER (accessed 30 October 2024).

Compagnucci, R., Agosta, E., Vargas, W. 2002. Climatic change and quasi-oscillations in central-west Argentina summer precipitation: main features and coherent behaviour with southern African region. *Climate Dynamics* 18, 421-435. https://doi.org/10.1007/s003820100183

de Santos Loureiro, N., de Azevedo Coutinho, M. 2001. A new procedure to estimate the RUSLE EI30 index, based on monthly rainfall data and applied to the Algarve region, Portugal. *Journal of Hydrology* 250 (1-4), 12-18. https://doi.org/10.1016/S0022-1694(01)00387-0

Di Leo, C.M., Aragón, A., Marlats, R.M., Bruno, J.E. 1999. Erosividad de las precipitaciones en Tandil, provincia de Buenos Aires. *Ciencia del Suelo* 17(2). http://sedici.unlp.edu.ar/handle/10915/159191

Di Leo, N., Barbona, I., Beltrán, C., Forgioni, F.P., Coronel, A., Jozami, E. 2024. Temporal variability of spatial patterns of correlations between summer rainfall and the Oceanic Niño Index in the Pampean region. *Science of The Total Environment* 955(176849). https://doi.org/10.1016/j.scitotenv.2024.176849

Diodato, N. 2004. Estimating RUSLE's rainfall factor in the part of Italy with a Mediterranean rainfall regime. *Hydrology and Earth System Sciences* 8(1), 103-107. https://doi.org/10.5194/hess-8-103-2004

Fang, B., Bevacqua, E., Rakovec, O., Zscheischler, J. 2024. An increase in the spatial extent of European floods over the last 70 years. *Hydrology and Earth System Sciences* 28(16), 3755-3775. https://doi.org/10.5194/hess-28-3755-2024

Fearnhead, P., Maidstone, R., Letchford, A. 2019. Detecting Changes in Slope with an L0 Penalty, *Journal of Computational and Graphical Statistics* 28(2), 265-275, http://doi.org/10.1080/10618600.2018.1512868

Forgioni, F.P., Coronel, A.S., Dickie, M.J., Jozami, E. 2023. Variabilidad de la relación entre el ONI y las precipitaciones del trimestre NDE en la provincia de Santa Fe. https://repositorio.inta.gob.ar/handle/20.500.12123/16537

Gabioud, E.A. 2018. *Regeneración de la estructura edáfica y su efecto sobre el ingreso del agua: evaluación del agregado de enmiendas en argiudoles bajo siembra directa.* Thesis of Master of Science, Universidad de Buenos Aires, Argentina. https://repositoriosdigitales.mincyt.gob.ar/vufind/Record/FAUBA_60b7e65ff7e9b21dad5eb8e52c407c59 (accessed 30 October 2024).

Government of Entre Ríos. 2019. *Plan de gestión integrada de riesgos en el sector agropecuario de la provincia de Entre Ríos*. https://www.argentina.gob.ar/sites/default/files/girsar_-_entre_rios_-_ppgira_ago19_compressed.pdf

Grimm, A.M., Barros, V.R., Doyle, M.E. 2000. Climate variability in southern South America associated with El Niño and La Niña events. *Journal of climate* 13(1), 35-58. https://doi.org/10.1175/1520-0442(2000)013<0035:CVISSA>2.0.CO;2

Halecki, W., Kruk, E., Ryczek, M. 2018. Evaluation of water erosion at a mountain catchment in Poland using the G2 model. *Catena* 164, 116-124. https://doi.org/10.1016/j.catena.2018.01.014

Henn, B., Newman, A.J., Livneh, B., Daly, C., Lundquist, J.D. 2018. An assessment of differences in gridded precipitation datasets in complex terrain. *Journal of Hydrology* 556, 1205-1219. https://doi.org/10.1016/j.jhydrol.2017.03.008

Informe del sector Agrícola, Provincia de Entre Ríos. 2023. Dirección General de Estadística y Censos, Gobierno de Entre Ríos. https://www.entrerios.gov.ar/dgec/wp-content/uploads/2022/12/Informe-agricola-2020.pdf (accessed 30 October 2024).

Intergovernmental Panel on Climate Change (IPCC). 2023. *Climate Change 2021 – The Physical Science Basis: Working Group I Contribution to the Sixth Assessment Report of the Intergovernmental Panel on Climate Change.* Cambridge, Cambridge University Press. https://doi.org/10.1017/9781009157896

Jozami, E., Constanzo, M., Coronel, A. 2015. Influencia de "El Niño-Oscilación Sur" sobre las precipitaciones en Paraná y Lucas González (Entre Ríos, Argentina). *Revista de Climatología* 15, 85-92.

López-Vicente, M., Álvarez, S. 2018. Stability and patterns of topsoil water content in rainfed vineyards, olive groves, and cereal fields under different soil and tillage conditions. *Agric. Water Manag.* 201, 167-176. https://doi.org/10.1016/j.agwat.2018.02.004

López-Vicente, M., Navas, A., Machín, J. 2008. Identifying erosive periods by using RUSLE factors in mountain fields of the Central Spanish Pyrenees. *Hydrology and Earth System Sciences* 12(2), 523-535. https://doi.org/10.5194/hess-12-523-2008

López-Vicente, M., Lana-Renault, N., García-Ruiz, J.M., Navas, A. 2011. Assessing the potential effect of different land cover management practices on sediment yield from an abandoned farmland catchment in the Spanish Pyrenees. *Journal of Soils and Sediments* 11, 1440- 1455. https://doi.org/10.1007/s11368-011-0428-2

López-Vicente, M., Pereira-Rodríguez, L., da Silva-Días, R., Raposo-Díaz, X., Wu, G.-L., Paz-González, A. 2023. Role of cultivars and grass in the stability of soil moisture and temperature in an organic vineyard. *Geoderma Regional* 33, e00631. https://doi.org/10.1016/j.geodrs.2023.e00631

Maggi, A.E. 2002. Una propuesta para predecir el factor de erosividad R para el centro y norte de la Argentina. *Revista de la Facultad de Agronomía* 22(2/3), 133-138. http://ri.agro.uba.ar/files/download/revista/facultadagronomia/2002maggiae.pdf (accessed 30 October 2024).

Magrin, G.O., Marengo, J.A., Boulanger, J.-P., Buckeridge, M.S., Castellanos, E., Poveda, G., Scarano, F.R., Vicuna, S. 2014a. Central and South América, in Barros, V.R., Field, C.B., Dokken, D.J., Mastrandrea, M.D., Mach, K.J., Bilir, T.E., Chatterjee, M., Ebi, K.L., Estrada, Y.O., Genova, R.C., Girma, B., Kissel, E.S., Levy, A.N., MacCracken, S., Mastrandrea, P.R., White, L.L. (Eds.), *Climate Change 2014: Impacts, Adaptation, and Vulnerability.* Cambridge University Press, Cambridge, UK and New York, NY, USA, pp. 1499-1566. https://www.ipcc.ch/site/assets/uploads/2018/02/WGIIAR5-Chap27_FINAL.pdf (accessed 30 October 2024).

Magrin, G.O, Travasso, M.I., Rodríguez, G. 2014b. Impactos del clima y medidas de adaptación del sistema productivo, in Pascale Medina, C., Zubillaga, M., Taboada, M.A. (Eds.), S*uelos, producción agropecuaria y cambio climático: avances en la Argentina*. Ministerio de Agricultura, Ganadería y Pesca, 1a ed. Ciudad Autónoma de Buenos Aires, Argentina. ISBN 978-987-1873-24-1. https://ubatic.agro.uba.ar/?q=node/79 (accessed 30 October 2024).

Ministerio de Economía. 2023. Informe productivo provincial- Entre Ríos. https://www.argentina.gob.ar/informes-provinciales/caracterizacion-productiva (accessed 18 November 2025).

Nearing, M.A., Yin, S.Q., Borrelli, P., Polyakov, V.O. 2017. Rainfall erosivity: An historical review. *Catena* 157, 357-362. https://doi.org/10.1016/j.catena.2017.06.004

NOAA. 2024. Download Climate Timeseries- Niño 3.4 SST Index. https://psl.noaa.gov/gcos_wgsp/Timeseries/Nino34/ (accessed 30 October 2024).

Nolz, R., Loiskandl, W. 2017. Evaluating soil water content data monitored at different locations in a vineyard with regard to irrigation control. *Soil Water Res.* 12 (3), 152- 160. http://doi.org/10.17221/9/2016-SWR

Nordlund, G., Tuomenvirta, H. 1998. Spatial variation in wet deposition amounts of sulphate due to stochastic variations in precipitation amounts. *Atmospheric Environment* 32 (17), 2913-2921. https://doi.org/10.1016/S1352-2310(98)00027-2

Panagos, P., Borrelli, P., Meusburger, K., Yu, B., Klik, A., Jae Lim, K., Yang, J., Ni, J., Miao, C., Chattopadhyay, N., Sadeghi, S., Hazbavi, Z., Zabihi, M., Larionov, G., Krasnov, S., Gorobets, A., Levi, Y., Erpul, G., Birkel, C., Hoyos, N., Naipal, V., Oliveira, P., Bonilla, C., Meddi, M., Nel, W., Al Dashti, H., Boni, M., Diodato, N., Van Oost, K., Nearing, M., Ballabio, C. 2017. Global rainfall erosivity assessment based on high-temporal resolution rainfall records. Scientific reports, 7(4175). https://doi.org/10.1038/s41598-017-04282-8

Panagos, P., Borrelli, P., Matthews, F., Liakos, L., Bezak, N., Diodato, N., Ballabio, C. 2022. Global rainfall erosivity projections for 2050 and 2070. *J. Hydrol.* 610, 127865. https://doi.org/10.1016/j.jhydrol.2022.127865

Peel, M.C., Finlayson, B.L., McMahon, T.A. 2007. Updated world map of the Köppen-Geiger climate classification. *Hydrol. Earth Syst. Sci*., 11, 1633-1644. https://doi.org/10.5194/hess-11-1633-2007

Penalba, O. C., Bettolli, M. L. 2011. Climate change impacts on atmospheric circulation and daily precipitation in the Argentine pampas region, in *Climate change - geophysical foundations and ecological effects* (pp. 137-156). IntechOpen. http://doi.org/10.5772/24163

Penalba, O.C., Vargas, W.M. 2004. Interdecadal and interannual variations of annual and extreme precipitation over central-northeastern Argentina. *International Journal of Climatology* 24(12), 1565-1580. http://doi.org/10.1002/joc.1069

Plan Mapa de Suelos. 1998. *Carta de Suelos de la República Argentina*. Departamento Paraná, Provincia de Entre Ríos, Serie Relevamiento de Recursos Naturales No 17 (pp. 1-114). INTA.

Podestá, G., Bert, F., Rajagopalan, B., Apipattanavis, S., Laciana, C., Weber, E., Easterling, W., Katz, R., Letson, D., Menendez, A. 2009. Decadal climate variability in the Argentine Pampas: regional impacts of plausible climate scenarios on agricultural systems. *Climate Research* 40(2-3), 199-210. https://doi.org/10.3354/cr00807

R Core Team, 2020. R: A language and environment for statistical computing. R Foundation for Statistical Computing, Vienna, Austria. [software] URL. https://www.R-project.org/

Ranzi, R., Le, T.H., Rulli, M.C. 2012. A RUSLE approach to model suspended sediment load in the Lo river (Vietnam): Effects of reservoirs and land use changes. *Journal of Hydrology* 422-423, 17-29. https://doi.org/10.1016/J.JHYDROL.2011.12.009

Re, M., Barros, V.R. 2009. Extreme rainfalls in SE South America. *Climatic Change* 96(1):119–136. https://doi.org/10.1007/s10584-009-9619-x

Renard, K.G., Foster, G.R., Weesies, G.A., McCool, D.K., Yoder, D.C. 1997. Predicting soil erosion by water: a guide to conservation planning with the Revised Universal Soil Loss Equation (RUSLE). US Department of Agriculture, *Agriculture Handbook* No.703, USDA, Washington DC. https://www3.epa.gov/npdes/pubs/ruslech2.pdf (accessed 30 October 2024).

Rojas, A.E., Conde, A.A. 1985. Estimación del factor "R" de la Ecuación Universal de Pérdida de Suelos para el centro-este de la República Argentina. *Ciencia del Suelo* 3(12), 85-94. https://www.suelos.org.ar/publicaciones/vol_3n1y2/Rojas.pdf (accessed 30 October 2024).

Saluso, J.H. 1999. *El Observatorio Agrometeorológico de la Estación Experimental Agropecuaria Paraná del INTA*. 32 p.

Saluso, J.H. 2008. Actualización del factor R de la ecuación universal de pérdida de suelo (EUPS) para una amplia zona del país. Período 1950/2005. *Agricultura sustentable. Serie Extensión* 51, 49-53.

Sasal, M.C., Castiglioni, M.G., Wilson, M.G. 2010. Effect of crop sequences on soil properties and runoff on natural-rainfall erosion plots under no tillage. *Soil and Tillage Research* 108(1-2), 24-29. https://doi.org/10.1016/j.still.2010.03.010

Sasal, María C., Wilson, M.G., Bedendo, D.J., Schulz, G.A. 2015. Provincia de Entre Ríos, in Casas R. R., Albarracín G. (Eds.), *El deterioro del suelo y del ambiente en la Argentina,* 1 ed., Vol. II. Centro para la Promoción de la Conservación del Suelo y del Agua. Fundación para la Educación, la Ciencia y la Cultura (FECIC). Ciudad autónoma de Buenos Aires, Buenos Aires, Argentina. ISBN 978-950-9149-39-7, pp. 111-120. https://repositorio.inta.gob.ar/xmlui/handle/20.500.12123/2138

Sasal, María C., Wilson, M.G., Bedendo, D.J., Caviglia, O.P., De Battista, J.J., Eclesia, R.P., Gabioud, E.A., Garciarena, N.A., Gvozdenovich, J.J., Ledesma, S., Lezana, L., Novelli, L.E., Oszust, J.D., Pioto, C., Rosenberger, J., Saluzzio, M.F., Sione, S.M.J., Seehaus, M., Van Opstal, N.V., Wingeyer, A.B. 2019. Provincia de Entre Ríos, in Casas, R. R., Damiano, F. (Eds.), *Manual de Buenas prácticas de conservación del suelo y del agua en áreas de secano.* Fundación para la Educación, la Ciencia y la Cultura (FECIC). Ciudad autónoma de Buenos Aires, Buenos Aires, Argentina. https://fecic.org.ar/wp-content/uploads/2023/06/Capitulo-Entre-Ri%CC%81os-para-web.pdf (accessed 30 October 2024).

Scott, A.J., Knott, M. 1974. A Cluster Analysis Method for Grouping Means in the Analysis of Variance. *Biometrics* 30(3), 507- 512. https://doi.org/10.2307/2529204

Suif, Z., Fleifle, A., Yoshimura, C., Saavedra, O. 2016. Spatio-temporal patterns of soil erosion and suspended sediment dynamics in the Mekong River Basin. *Science of The Total Environment* 568, 933-945. https://doi.org/10.1016/j.scitotenv.2015.12.134

Tsitsagi, M., Berdzenishvili, A., Gugeshashvili, M. 2018. Spatial and temporal variations of rainfall-runoff erosivity (R) factor in Kakheti, Georgia. *Annals of Agrarian Science* 16(2), 226-235. https://doi.org/10.1016/j.aasci.2018.03.010

USDA-Agricultural Research Service. 2013. Revised Universal Soil Loss Equation Version 2 (RUSLE 2). Washington DC. https://www.ars.usda.gov/southeast-area/oxford-ms/national-sedimentation-laboratory/watershed-physical-processes-research/research/rusle2/revised-universal-soil-loss-equation-2-rusle2-documentation (accessed 30 October 2024).

Vachaud, G., Passerat de Silans, A., Balabanis, P. Vauclin, M. 1985. Temporal stability of spatially measured soil water probability density function. *Soil Science Society of America Journal* 49(4), 822-828. https://doi.org/10.2136/sssaj1985.03615995004900040006x

Wang, W., Yin, S., Xie, Y., Nearing, M.A. 2019. Minimum inter-event times for rainfall in the eastern monsoon region of China. *Transactions of the ASABE* 62 (1), 9-18. https://doi.org/10.13031/trans.12878

Wei, L., Dong, J., Gao, M., Chen, X. 2017. Factors controlling temporal stability of surface soil moisture: a watershed-scale modelling study. *Vadose Zone J.* 16 (10). https://doi.org/10.2136/vzj2016.12.0132

Wingeyer, A.B., Maffini, G., Gabioud, E.A., Seehaus, M.S., Garciarena, N. 2022. Actualización de los promedios históricos de temperatura y precipitaciones para la zona de la EEA Paraná del INTA. *Serie Extensión INTA Paraná* 87, 52-56. http://hdl.handle.net/11336/200497

Zhang, Y., Li, H., Sun, Y., Zhang, Q., Liu, P., Wang, R., Li, J. 2022. Temporal stability analysis evaluates soil water sustainability of different cropping systems in a dryland agricultural ecosystem. *Agric. Water Manag.* 272, 107834. http://doi.org/10.1016/j.agwat.2022.107834

Zhao, Y., Peth, S., Wang, X.Y., Lin, H., Horn, R. 2010. Controls of surface soil moisture spatial patterns and their temporal stability in a semi-arid steppe. *Hydrol. Process.* 24, 2507-2519. https://doi.org/10.1002/hyp.7665

Supplementary material

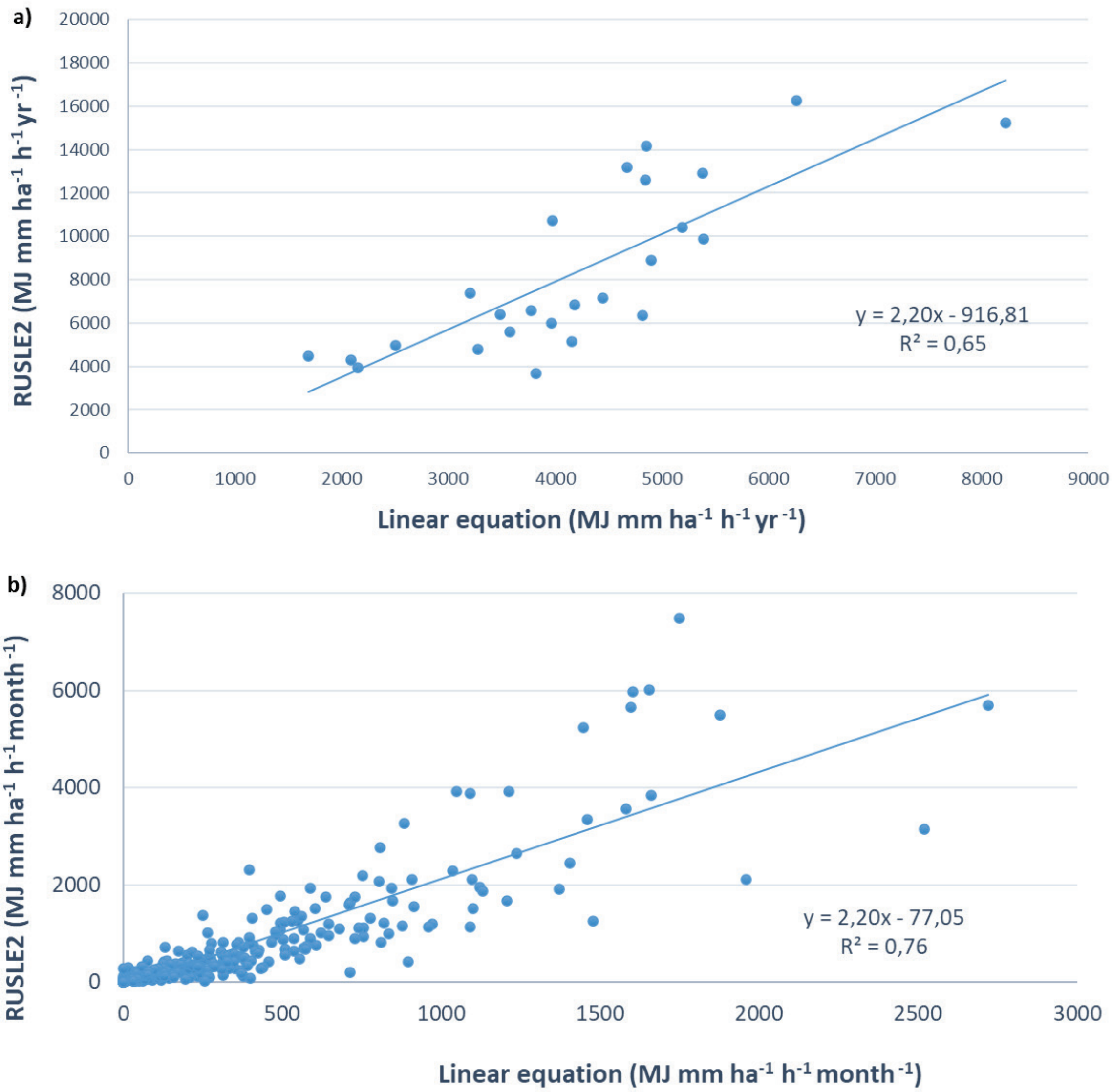

SM1. Annual (a) and monthly (b) factor R (1999-2023) - RUSLE2 (Eq. (1) and (2)) vs. linear (Eq. (3)) approaches.

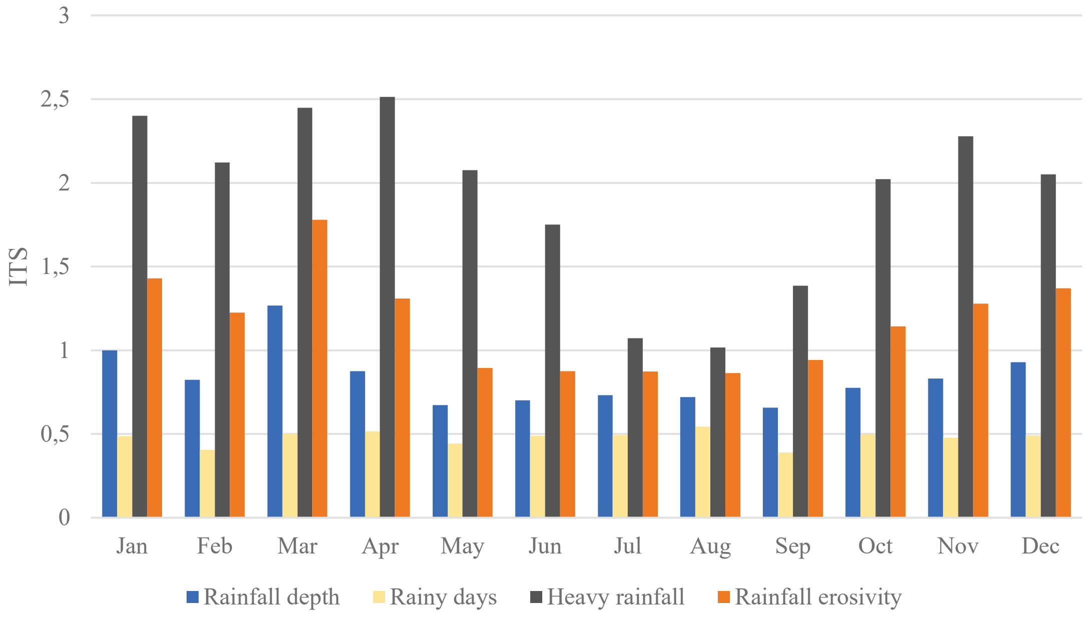

SM2. Monthly values of the index of temporal stability (ITS) of rainfall depth (a); rainy days (b); heavy rainfall (c); and rainfall erosivity (d) for the 90-year study period (1934-2023).

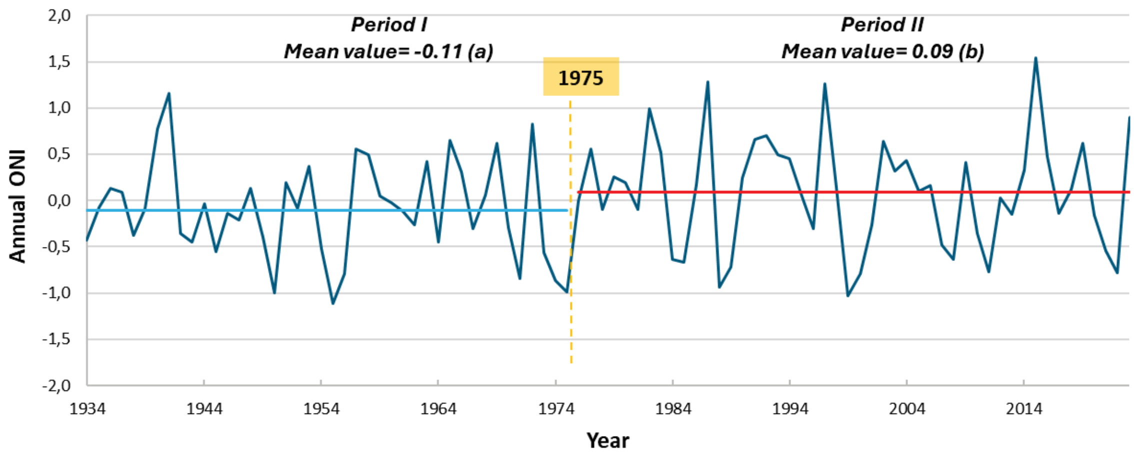

SM3. Annual values (1934-2023) of the Oceanic Niño Index (ONI) and means in period I and period II according to breakpoint (breakdate in an orange-filled box). Different letters indicate significant differences between the analysis periods (ANOVA test DGC, p < 0,10).